# Supplementary Information

# Pyridine-copper (II) formates for the generation of high conductivity copper films at low temperatures

C. Paquet[a], T. Lacelle[a], B. Deore[a], A. J. Kell[a], X. Liu[a], I. Korobkov[b], P. R.L. Malenfant[a]

## Content



## 1. Experimental

### a) Materials

Copper (II) formate hydrate was purchased from Strem Chemicals Inc. All amines and solvents were purchased from Sigma-Aldrich and were used as is. Melinex ST505™ (PET) was purchased from Tekra while Kapton HPPST (polyimide) was purchased from Dupont. To prepare the amino cupric formates, copper (II) formate was first ground into a fine powder. Copper (II) formate was then suspended in acetonitrile and stirred. Amines in a molar ratio of 2:1 amine:copper formate were added to the

suspension, turning the suspension into a dark blue solution. The solution was stirred for approximately 30 minutes, filtered and crystallized at -4°C. The crystals were isolated and dried under vacuum. Yields were approximately 40%-80%. XRD and elemental analysis of the EtHex shows the compound crystallized with a water molecule. The 3ButPy compound could not be crystallized and as a result, their solutions were rotary evaporated after the filtration step. Films of the amino cupric formates were prepared by first diluting the compound in anisole to make a thick paste (~1g/mL). Label tape was used to form a mask of 1 cm x1 cm squares on Melinex and Kapton. The molecular copper paste was doctor bladed to form square films. Films were left for 10-20 minutes prior to heating them to the temperatures described in the heating profiles of Figure SI_3. The resulting films were from 3 to 11 μm in thickness.

b) **Instrumentation.**

Solutions of Octyl, EtHex, tButPy and 3ButPy in toluene were characterized by a Cary 5000 spectrophotometer from Varian. Pellets of the compounds in KBr were prepared and analyzed on a Thermo Electron Coorporation FTIR spectrometer. The CHNS elemental analysis was done using the Elementar Vario EL Cube analyzer. Approximately 10mg of sample was weighed and wrapped in a tin boat prior to the analysis. The catalytic combustion was carried out at 1200°C for about 120s. Subsequently, the reduction of the combustion gases on hot copper is carried out in a second furnace. The gas mixture was separated in its components via three columns by purge and trap chromatography and is subsequently fed into a thermal conductivity detector (TCD). Elemental analysis was done in triplicates. Powder XRD data were collected with a Bruker D8 Advanced diffractometer. Two-theta angles of 30-90° were acquired with an increment of 0.0131034 and a scan speed of 1.2 sec/step. Optical images were taken of the compounds heated on a Fisher Scientific melting point apparatus using a Dino-lite camera. Scanning electron microscopy (SEM) images were acquired with a JEOL JSM840A at an accelerating voltage of 20 kV. Coupled analyses of thermogravimetry (TG) and absorption

spectroscopy in the mid-infrared region were performed on a Netzsch TG 209 F1 Iris R coupled to a Bruker Tensor 27 Fourier transform infrared (FTIR) spectrometer via a TGA A588 TGA-IR module. The system was run with BOC HP argon (grade 5.3) gas and residual oxygen was trapped with a Supelco Big-Supelpure oxygen/water trap. Transfer lines between the TG instrument and FTIR spectrometer were heated to a temperature of 200 ◦C. The curves in Figure 4 were acquired by integrating the FTIR signal in a range of frequencies associated with either the vibration mode of $CO_2$ or a methylene bending or ring stretching mode of amines or pyridine as a function of temperature. Thus for the $CO_2$ curve in Figure 4a, the absorbance between 2200-2450 $cm^{-1}$ was integrated at each temperature and plotted as a function of temperature thus representing the desorption of $CO_2$. The curves in Figure 4b were acquired by integrating the frequencies at 1440-1480 $cm^{-1}$ for amines or 1590-1610 $cm^{-1}$ for pyridine derivatives at each temperature and thus illustrate the release of amines or the pyridine derivatives as a function of temperature. Mass spectrometry

**c) Resistivity Measurement**

The resistance was measured with a 4-point probe (SP4 four-point-probe type by Lucas Labs) using a source-meter in the current mode (Keithly 220 programmable current source) and measuring voltage with a HP 3478A multimeter. A current of 100mV was applied on the outer probes and the voltage was measured on the inner probes. The sheet resistance was calculated from the resistance using a correction factor that varied from 3.11 to 4.22, depending on the diameter of the copper film (given the probe spacing of 1.016 mm). The resistivity was calculated from the sheet resistance ($R_{sh}$) by using $R_{sh}=\rho/h$, where $\rho$ is the resistivity and h is the height of the sample. A CT-100 optical profiler by Cyber Technologies was used to determine film thickness and calculate volume resistivity.

**d) X-ray Crystallography.**

Data collection results for compounds *tButPy* represent the best data set obtained in several trials. The crystal was mounted on thin glass fibers using paraffin oil. Prior to data collection crystals were cooled to 200.15 °K. Data were collected on a Bruker AXS SMART single crystal diffractometer equipped with a sealed Mo tube source (wavelength 0.71073 Å) APEX II CCD detector. Raw data collection and processing were performed with APEX II software package from BRUKER AXS. [ref 1] Due to low unit cell symmetry in order to ensure adequate data redundancy, diffraction data were collected with a sequence of 0.3° $\omega$ scans at 0, 90, 180 and 270° in $\varphi$. Initial unit cell parameters were determined from 60 data frames with 0.3° $\omega$ scan each, collected at the different sections of the Ewald sphere. Semi-empirical absorption corrections based on equivalent reflections were applied.[ref 2] Diffraction reflection intensities and unit-cell parameters were consistent with triclinic $\mathbf{P\bar{1}}$ (№2) space group. Solution in the centrosymmetric space group yielded chemically reasonable and computationally stable results of refinement. The structure was solved by direct methods, completed with difference Fourier synthesis, and refined with full-matrix least-squares procedures based on $F^2$.

Structure solution for *tButPy* revealed structural model containing one molecule of the target compound per asymmetric unit located in the inversion center symmetry element of the space group. Structural model was refined with full set of anisotropic thermal displacement parameters for all non-hydrogen atoms, generating acceptable values of thermal motion coefficients and stable refinement results.

All hydrogen atomic positions were calculated based on the geometry of related non-hydrogen atoms. All hydrogen atoms were treated as idealized contributions during the refinement. All scattering factors are contained in several versions of the SHELXTL program library, with the latest version used being v.6.12[ref 3]

### e) Magnetic susceptibility by NMR

The magnetic susceptibilities of the compounds were determined using the Evans method at 25°C. A weight of approximately 7 mg of copper compound was accurately weighed and dissolved in 0.970 mL of $CDCl_3$ and 0.030 mL of *t*-butanol. The solution was transferred to a melting point capillary and the capillary was flame-sealed. A standard solution of in 0.970 mL of $CDCl_3$ and 0.030 mL of *t*-butanol was prepared and transferred to a NMR tube. The frequency difference between the t-butanol signal and that of the copper compound was determined using a Bruker AV-III 400 high resolution NMR spectrometer.

The magnetic susceptibilities were calculated using a simplified equation[4]:

$$\chi_{mass} = 3\Delta f/4\pi fm + \chi_0 \qquad (eq.1)$$

- $\chi_{mass}$ is mass susceptibility in $cm^3g^{-1}$
- $\Delta f$ is measured freq difference in Hz
- f is spectrometer frequency, ($400.132471 \times 10^6$ Hz)
- m is mass of paramagnetic substance in $g \cdot cm^{-3}$ i.e. concentration in g/mL
- $\chi_0$ is mass susceptibility of $CDCl_3$ in $cm^3g^{-1}$ ($-0.7\ 4 \times 10^{-6}$ $cm^3g^{-1}$)

## 2. UV-VIS, FT-IR and Elemental Analysis of Octyl, EtHex, 3ButPy and tButPy

### UV-Vis spectroscopy

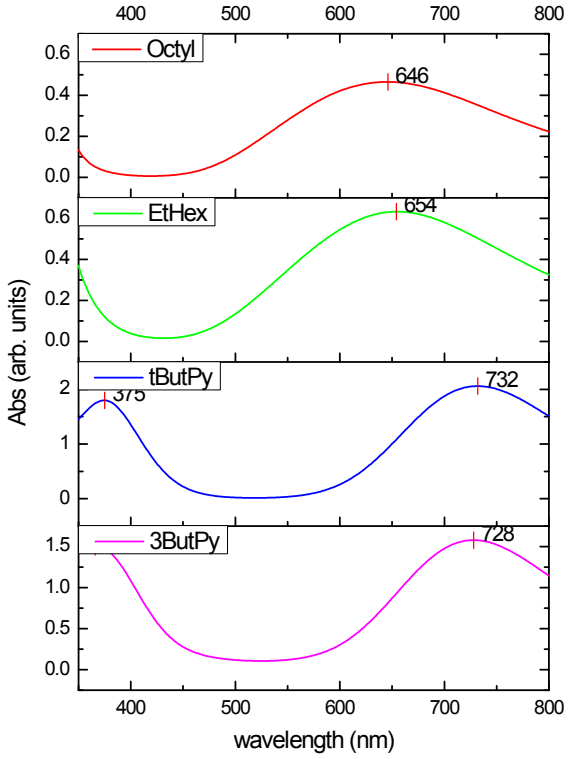


**Figure SI_1**. UV-VIS spectrum of Octyl (4.8mg/mL), EtHex (4.7mg/mL), tButPy (5.1mg/mL) and 3ButPy (3.7mg/mL).

## FT-IR spectroscopy

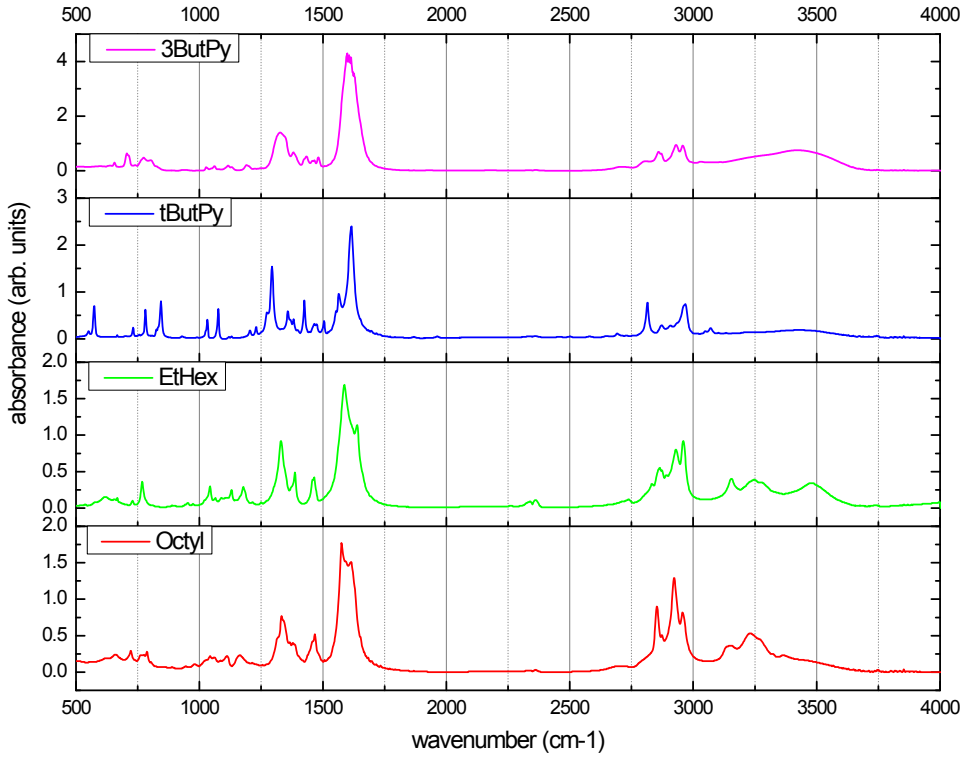


**Figure SI_2**. FTIR spectra of Octyl, EtHex, tButPy and 3ButPy

## Elemental analysis

**Table SI_1.** Calculated and experimental percent weight of N, C, H and S of the copper formate compounds.

| Sample | Weight [mg] | N [wt%] | | C [wt%] | | H [wt%] | | S [wt%] | |
|---|---|---|---|---|---|---|---|---|---|
| | | measured | calculated | measured | calculated | measured | calculated | measured | calculated |
| (2:1) Octyl | 11.116 | 6.75 | 6.80 | 52.74 | 52.47 | 10.24 | 9.78 | 0.099 | 0 |
| (2:1) EtHex·$H_2O$ | 10.437 | 6.45 | 6.51 | 50.54 | 50.27 | 10.43 | 9.84 | 0.018 | 0 |
| (2:1)tButPy | 10.533 | 6.51 | 6.61 | 56.71 | 56.66 | 7.10 | 6.66 | 0.007 | 0 |
| (1.4:1) 3ButPy | 10.699 | 5.78 | 5.72 | 50.92 | 51.14 | 6.39 | 5.94 | 0.002 | 0 |

## Magnetic susceptibilities

The magnetic susceptibilities of the compounds at 25°C determined by the Evans method are shown in Table S1-2. The values of $2.4 \times 10^{-4}$ and $7.9 \times 10^{-4}$ $cm^3/mol$ are similar to those found previously for copper formate-pyridine compounds of ($4.5\text{-}5.0 \times 10^{-4}$ $cm^3/mol$). [5]

**Table SI-2.** The measured frequency shift, concentration, and the calculated mass and molar magnetic susceptibilities of the copper formate compounds at 25°C.

| sample | Δf (hz) | m (g/mL) | $\chi_{mass}$ ($cm^3 \cdot g^{-1}$) | M (g/mol) | $\chi_{mol}$ ($cm^3 \times mol^{-1}$) |
|---|---|---|---|---|---|
| Octyl | 40.683 | 0.0075 | 2.5E-06 | 412.102 | 1.0E-03 |
| EtHex | 32.362 | 0.0075 | 1.8E-06 | 412.102 | 7.6E-04 |
| 3ButPy | 15.901 | 0.0073 | 5.6E-07 | 423.993 | 2.4E-04 |
| tButPy | 33.281 | 0.0076 | 1.9E-06 | 423.993 | 7.9E-04 |

## 3. Mass spectrometry

The copper (II) formate compounds were analyzed by LTQ-Orbitrap mass spectrometry. The goal was to establish which species were present in the samples via mass spectrometry. The core functionality was expected to consist of a copper atom with two covalently bonded formate groups. Mass spectrometry was used to elucidate the number or amines coordinated to the copper as shown below:

1) Octyl 2 amine: $C_{18}H_{40}N_2O_4Cu$ 3 amine: $C_{26}H_{59}N_3O_4Cu$
2) EtHex 2 amine: $C_{18}H_{40}N_2O_4Cu$ 3 amine: $C_{26}H_{59}N_3O_4Cu$
3) 3-ButPy 2 amine: $C_{20}H_{28}N_2O_4Cu$ 3 amine: $C_{29}H_{41}N_3O_4Cu$
4) t-ButPy 2 amine: $C_{20}H_{28}N_2O_4Cu$ 3 amine: $C_{29}H_{41}N_3O_4Cu$

**Experimental:**

Solutions of each Cu compound were prepared at approximately 1 mg/mL. 3-ButPy, and t-ButPy samples dissolved readily ion methanol. Octyl amine and EtHex amine samples did not dissolve well in methanol, however the addition of 0.1% formic acid resulted in full dissolution of the samples.

Each sample was infused (5 µL/min) into an LTQ Orbitrap mass spectrometer equipped with an electrospray ionization source. Full scan spectra were acquired for 30 seconds over a range of m/z 50-2000. MSMS spectra were acquired for 30 seconds over a range specific to each parent ion. The mass spectrometer was calibrated each day before use to ensure the collection of accurate mass data. The mass spectrometer parameters are listed below:

**MS Tune File Conditions: LTQ - Orbitrap:**

| Parameter | Setting |
|---|---|
| Ion Source | HESI |
| Probe Position | B, 1.75 |
| ISV (V) | 4000 |
| Sheath Gas | 5 |
| Aux Gas | 5 |
| Sweep Gas | 0 |
| Capillary Temp. (°C) | 50 |
| Heater Temp. (°C) | 275 |
| Capillary (V) | 15 |
| Tube lens (V) | 110 |

**MS Conditions: LTQ - Orbitrap:**

| Parameter | Setting |
|---|---|
| Analyzer | FTMS |
| Mass range | Normal |
| Resolution | 60 000 / 15 000 |
| Scan Type | Full / MSMS |
| Polarity | Positive |
| Data Type | Profile |
| Scan ranges (amu) | 50-2000 |
| Acquire Time (min) | 0.5 |

**Results:**

1) ***Octyl***:
   There is evidence of a di-amine copper complex in this sample. While the molecular ion at 412 is not observed, a series of losses are observed; one formate loss (366 ion), two formate loss (321 ion), one formate + one octylamine sidechain loss (237 ion) and two formate + one octylamine sidechain loss (192 ion). The exact masses of the observed ions are consistent with the molecular formulae. The formate groups appear to be lost readily, so it is possible that the intact di-amine copper formate exists but does not survive ionization. This cannot be confirmed.

   There are also several higher mass, lower intensity peaks, which may be due to dimeric or trimeric copper compounds based on the isotope pattern. This cannot be confirmed and may be an ionization phenomenon. MS-MS on these ions gives product ions consistent with the bis(octylamines) copper (II) formate structure.

   The corresponding ions of the tris(octylamines) copper (II) formate are not observed.

2) ***EtHex***:
   This sample behaved very similar to the octylamine sample, as expected. There is evidence of a di-amine copper complex in this sample. While the molecular ion at 412 is not observed, a series of losses are observed; one formate loss (366 ion), two formate loss (321 ion), one formate + one 2-ethyl-1-hexylamine sidechain loss (237 ion) and two formate + one 2-ethyl-1-hexylamine sidechain loss (192 ion). The exact masses of the observed ions are consistent with the molecular formulae. The formate groups appear to be lost readily, so it is possible that the intact di-amine copper formate exists but does not survive ionization. This cannot be confirmed.

   There are also several higher mass, lower intensity peaks, which may be due to dimeric or trimeric copper compounds based on the isotope pattern. This cannot be confirmed and may be an ionization phenomenon. MS-MS on these ions gives product ions consistent with the bis(2-ethyl-1-hexylamine) copper (II) formate structure.

   The corresponding ions of tris(2-ethyl-1hexylamine) copper (II) formate complex are not observed.

3) ***3ButPy***:
   There is evidence of a di-pyridine copper complex in this sample. While the molecular ion at 424 is not observed, a series of losses are observed; one formate loss (378 ion), two formate loss (333 ion), one formate + one 3-butylpyridine sidechain loss (243 ion) and two formate + one 3-butylpyridine sidechain loss (198 ion). The exact masses of the observed ions are consistent with the molecular formulae. The formate groups appear to be lost readily, so it is possible that the intact di-pyridine copper formate exists but does not survive ionization. This cannot be confirmed.

There are also several higher mass, lower intensity peaks, which may be due to dimeric or trimeric copper compounds based on the isotope pattern. This cannot be confirmed and may be an ionization phenomenon. MS-MS on these ions gives product ions consistent with the bis(3-butylpyridine) copper formate structure.

The corresponding ions for tris(3-butylpyridine) copper (II) formate are not observed.

4) ***tButPy***:
There is evidence of a di-pyridine copper complex in this sample. While the molecular ion at 424 is not observed, a series of losses are observed; one formate loss (378 ion), two formate loss (333 ion), one formate + one tert-butylpyridine sidechain loss (243 ion) and two formate + one tert-butylpyridine sidechain loss (198 ion). The exact masses of the observed ions are consistent with the molecular formulae. The formate groups appear to be lost readily, so it is possible that the intact di-amine copper formate exists but does not survive ionization. This cannot be confirmed.

There are also several higher mass, lower intensity peaks, which may be due to dimeric or trimeric copper compounds based on the isotope pattern. This cannot be confirmed and may be an ionization phenomenon. MS-MS on these ions gives product ions consistent with the bis(tert-butylpyridine) copper (II) formate structure. The corresponding ions of the tris(tert-butylpyridine) copper (II) formate are not observed.

Overall, the samples provide a complex mass spectrum. Not all of the major observed ions have been identified and it is not possible to confirm whether or not the observed ions are distinct species existing in the sample or if they are produced in the ionization process of the mass spectrometer.

LC-MS was attempted to separate potential distinct species prior to introduction to the mass spectrometer, however the limited efforts were not successful.

## 4. Heating Profiles

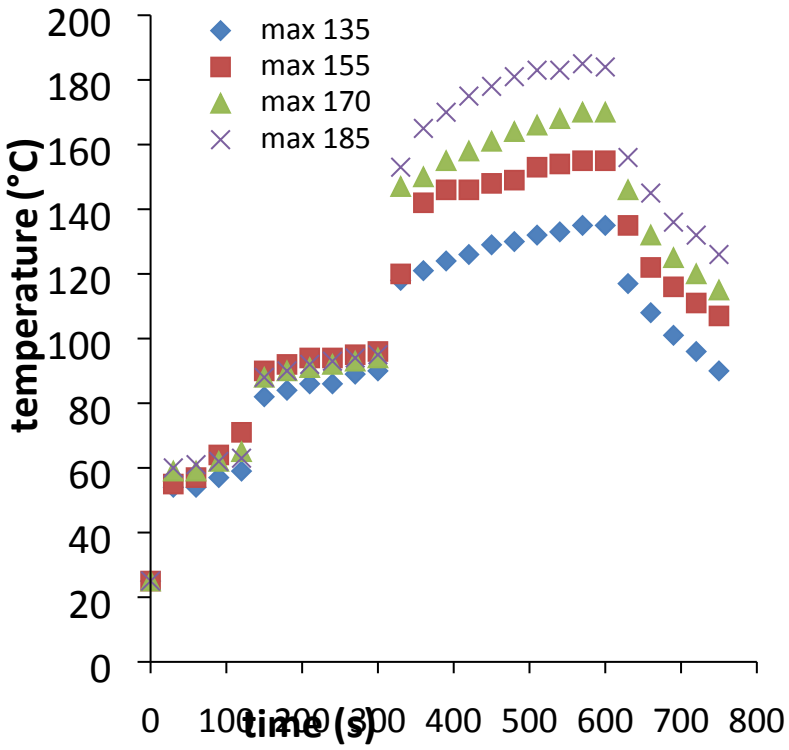


**Figure SI_3**. Temperature program used to sinter the molecular copper inks.

## 5. Thermal stability of PET

The temperature stability of Melinex ST505™ (PET) was tested by heating bare pieces of substrates under the same temperature programs used to sinter the molecular copper inks. The transmission of light at 400nm was measured for each substrate after heat treatment. The results, found in Figure SI-4, show that heating to 135°C for 4.5 minutes does not change the optical properties of the substrate in comparison to an untreated Melinex sample. Thermal treatment at or above 155°C causes the substrate to decrease in transmission.

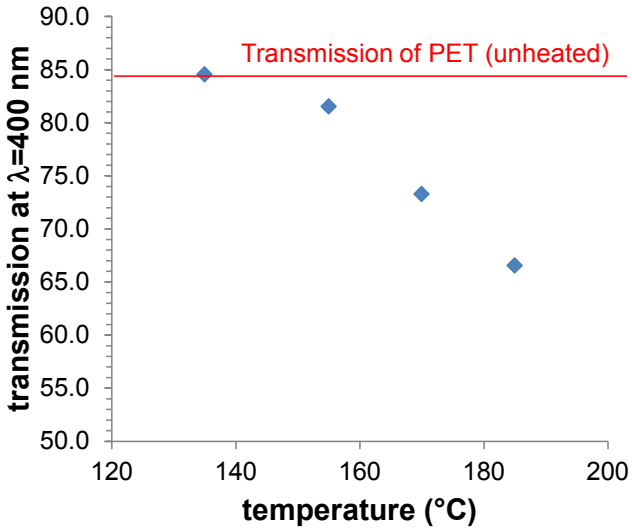


**Figure SI_4.** Transmission of 400 nm light of heat treated Melinex substrates.

## 6. FTIR spectra

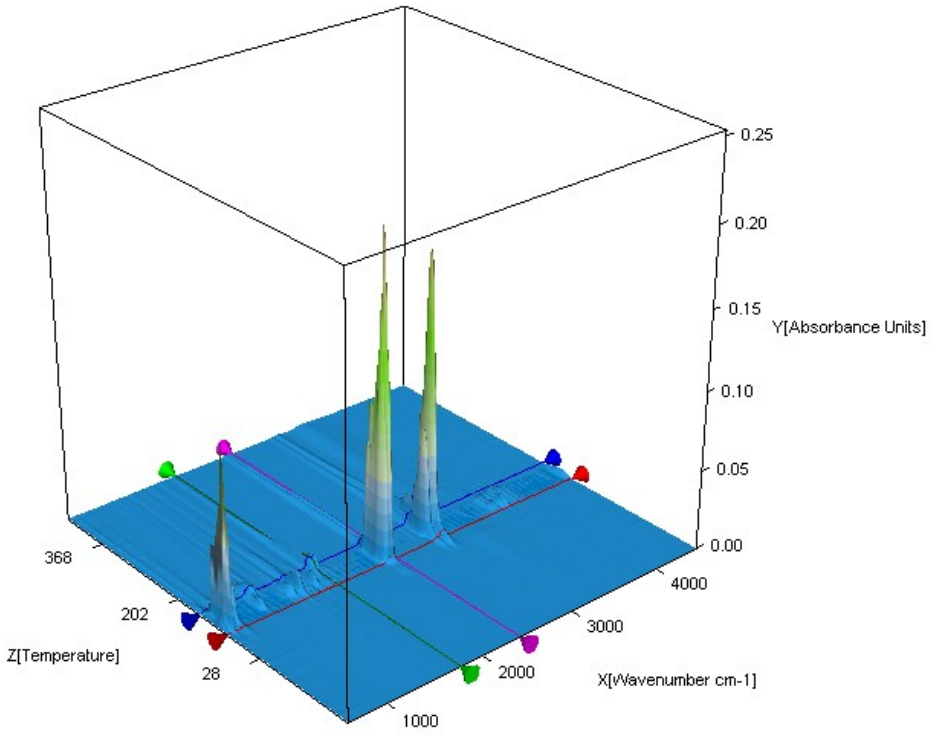


**Figure SI_5**. A three dimensional plot of the FT-IR absorbances as a function of temperature and wavenumber of *Octyl*.

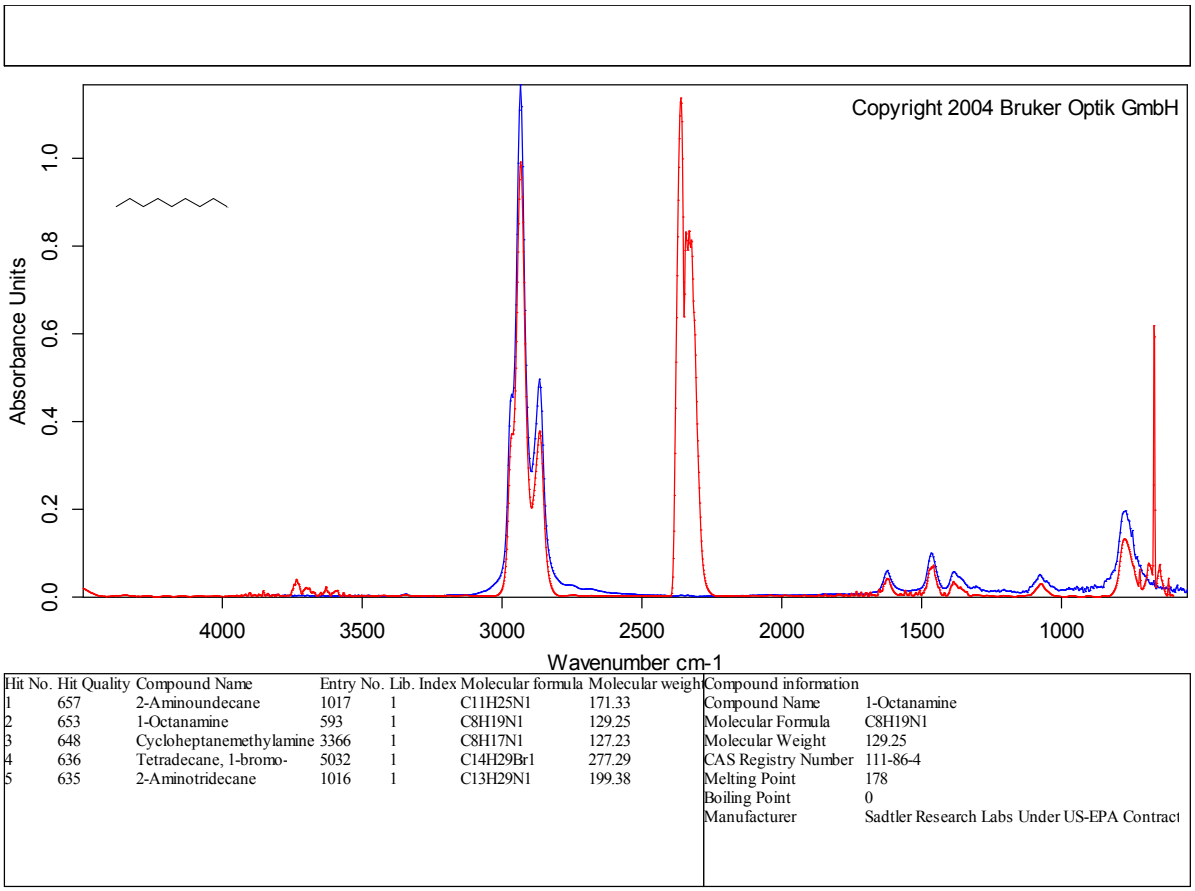


| Hit No. | Hit Quality | Compound Name | Entry No. | Lib. Index | Molecular formula | Molecular weight |
|---|---|---|---|---|---|---|
| 1 | 657 | 2-Aminoundecane | 1017 | 1 | C11H25N1 | 171.33 |
| 2 | 653 | 1-Octanamine | 593 | 1 | C8H19N1 | 129.25 |
| 3 | 648 | Cycloheptanemethylamine | 3366 | 1 | C8H17N1 | 127.23 |
| 4 | 636 | Tetradecane, 1-bromo- | 5032 | 1 | C14H29Br1 | 277.29 |
| 5 | 635 | 2-Aminotridecane | 1016 | 1 | C13H29N1 | 199.38 |

| Compound information | |
|---|---|
| Compound Name | 1-Octanamine |
| Molecular Formula | C8H19N1 |
| Molecular Weight | 129.25 |
| CAS Registry Number | 111-86-4 |
| Melting Point | 178 |
| Boiling Point | 0 |
| Manufacturer | Sadtler Research Labs Under US-EPA Contract |

**Page 1/1**

**Figure SI_6**: FTIR spectra of the volatile products resulting from the decomposition of *Octyl* at 118°C (red curve). The spectrum of octylamine (blue curve) is included as a visual aid.

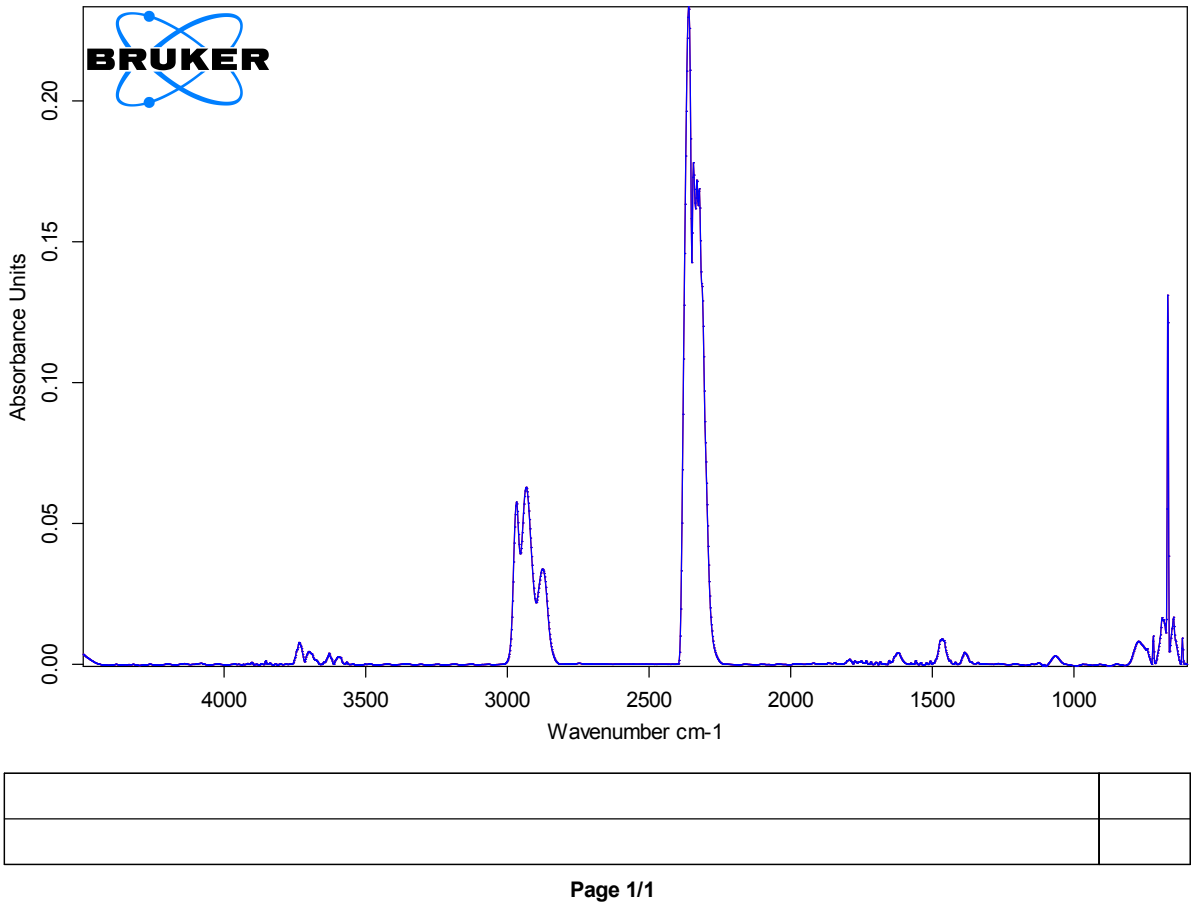


**Figure SI_7**: FTIR spectra of the volatile products resulting from the decomposition of *EtHex* at 111°C.

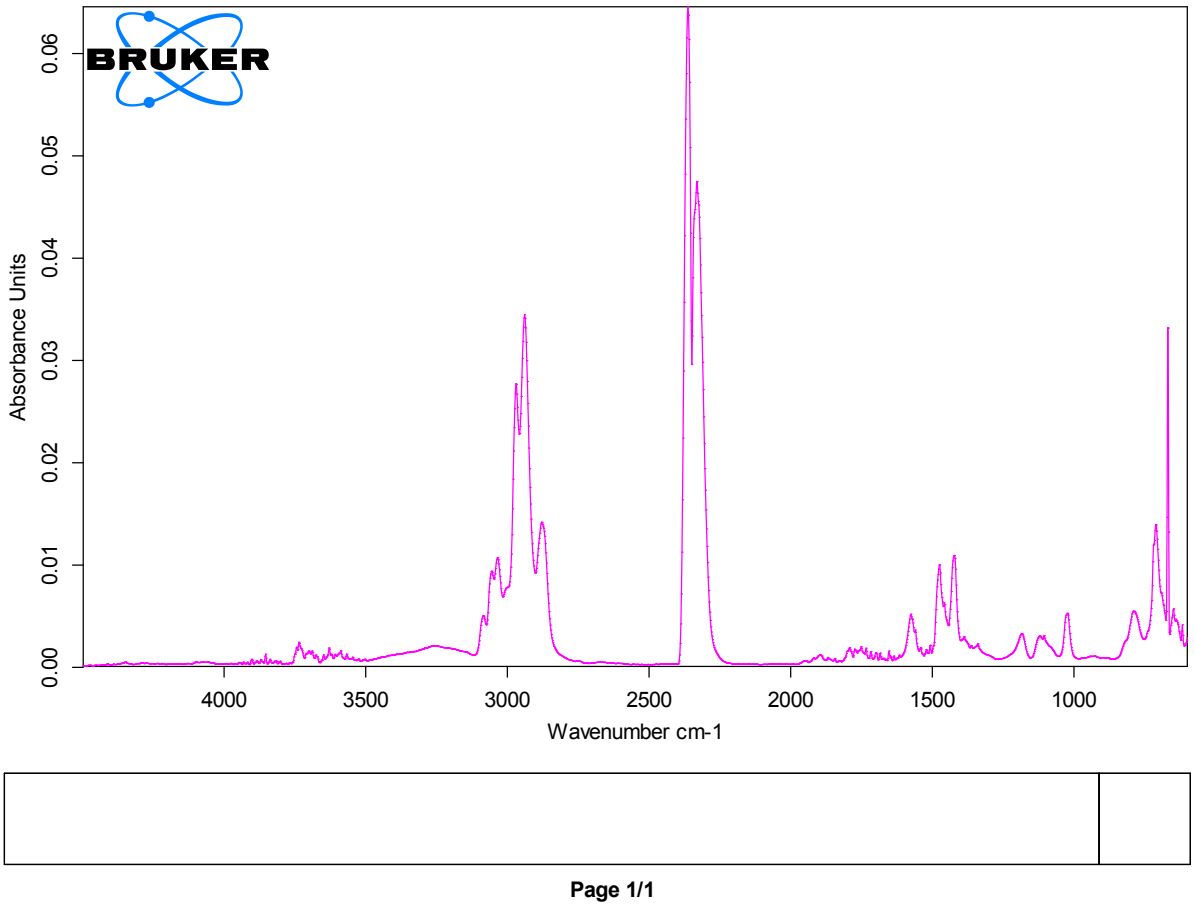


**Figure SI_8**: FTIR spectra of the volatile products resulting from the decomposition of*3ButPy* at 91°C.

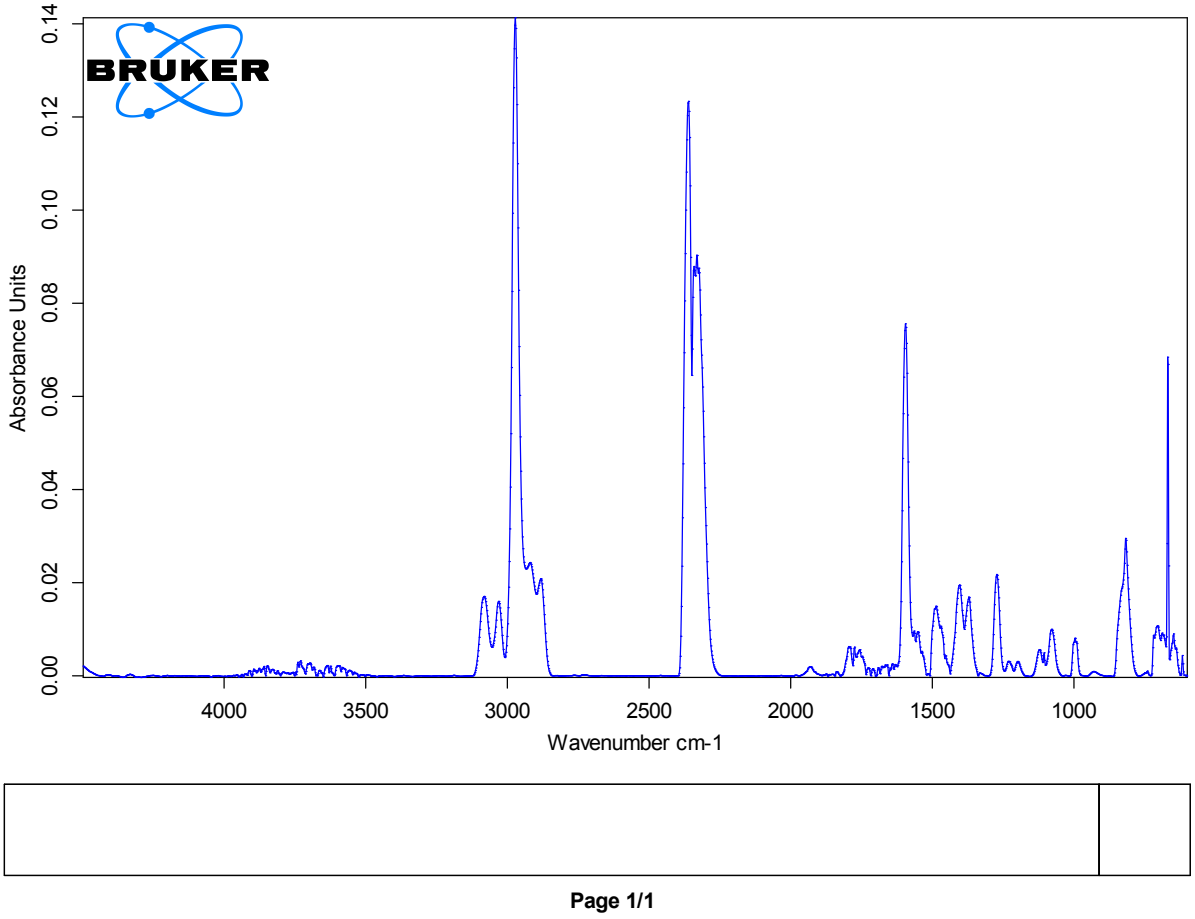


**Figure SI_9**: FTIR spectra of the volatile products resulting from the decomposition of *tButPy* at 108°C.

## 7. SEM

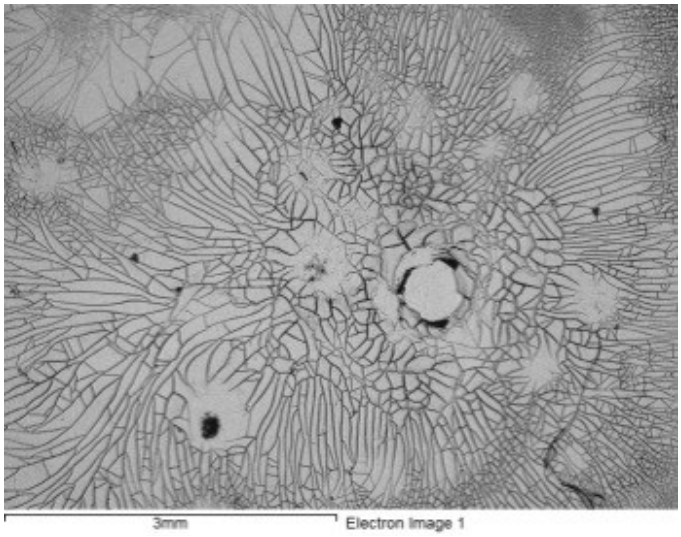


**Figure SI_10:** SEM image of a film made from tButPy illustrating the cracks formed during sintering.

## 8. XRD data of tButPy

Table 1. Crystal data and structure refinement for tButPy.

| | | | |
|---|---|---|---|
| 3. | Identification code | tButPy | |
| 4. | Empirical formula | C20 H28 Cu N2 O4 | |
| 5. | Formula weight | 423.98 | |
| 6. | Temperature | 200(2) K | |
| 7. | Wavelength | 0.71073 Å | |
| 8. | Crystal system | Triclinic | |
| 9. | Space group | P -1 | |
| 10. | Unit cell dimensions | a = 7.5787(2) Å | α= 72.4479(15)°. |
| 11. | | b = 8.0875(2) Å | β= 68.0319(15)°. |
| 12. | | c = 9.6138(3) Å | γ = 85.0439(16)°. |
| 13. | Volume | 520.80(3) $Å^3$ | |
| 14. | Z | 1 | |
| 15. | Density (calculated) | 1.352 $Mg/m^3$ | |
| 16. | Absorption coefficient | 1.075 $mm^{-1}$ | |
| 17. | F(000) | 223 | |
| 18. | Crystal size | 0.380 x 0.260 x 0.200 $mm^3$ | |
| 19. | Theta range for data collection | 2.388 to 28.365°. | |
| 20. | Index ranges | -10<=h<=10, -10<=k<=10, -12<=l<=12 | |
| 21. | Reflections collected | 5143 | |
| 22. | Independent reflections | 2524 [R(int) = 0.0121] | |
| 23. | Completeness to theta = 25.242° | 97.5 % | |
| 24. | Absorption correction | Semi-empirical from equivalents | |
| 25. | Max. and min. transmission | 0.7457 and 0.6130 | |
| 26. | Refinement method | Full-matrix least-squares on $F^2$ | |
| 27. | Data / restraints / parameters | 2524 / 0 / 124 | |
| 28. | Goodness-of-fit on $F^2$ | 1.052 | |
| 29. | Final R indices [I>2sigma(I)] | R1 = 0.0251, wR2 = 0.0717 | |
| 30. | R indices (all data) | R1 = 0.0259, wR2 = 0.0722 | |
| 31. | Extinction coefficient | n/a | |
| 32. | Largest diff. peak and hole | 0.473 and -0.291 $e.Å^{-3}$ | |

Table 2. Atomic coordinates ( x $10^4$) and equivalent isotropic displacement parameters ($Å^2$x $10^3$) for tButPy. U(eq) is defined as one third of the trace of the orthogonalized $U^{ij}$ tensor.

| | x | y | z | U(eq) |
|---|---|---|---|---|
| Cu(1) | 10000 | 5000 | 0 | 28(1) |
| O(1) | 8651(1) | 6044(1) | -1432(1) | 36(1) |
| O(2) | 10577(2) | 4376(2) | -2777(2) | 54(1) |
| N(1) | 8247(1) | 2903(1) | 956(1) | 29(1) |
| C(1) | 9331(2) | 5438(2) | -2602(2) | 39(1) |
| C(2) | 6406(2) | 3038(2) | 1158(1) | 30(1) |
| C(3) | 5147(2) | 1629(2) | 1829(1) | 29(1) |
| C(4) | 5785(2) | -36(2) | 2313(1) | 27(1) |
| C(5) | 7719(2) | -170(2) | 2070(2) | 33(1) |
| C(6) | 8883(2) | 1302(2) | 1411(2) | 34(1) |
| C(7) | 4468(2) | -1644(2) | 3099(2) | 33(1) |
| C(8) | 2463(2) | -1246(2) | 3143(3) | 70(1) |
| C(9) | 5251(2) | -2989(2) | 2188(2) | 46(1) |
| C(10) | 4475(3) | -2453(2) | 4754(2) | 54(1) |

Table 3. Bond lengths [Å] and angles [°] for tButPy.

| | | |
|---|---|---|
| 53. | | |
| 54. | Cu(1)-O(1) | 1.9635(9) |
| 55. | Cu(1)-O(1)#1 | 1.9635(9) |
| 56. | Cu(1)-N(1) | 2.0052(10) |
| 57. | Cu(1)-N(1)#1 | 2.0052(10) |
| 58. | O(1)-C(1) | 1.2756(19) |
| 59. | O(2)-C(1) | 1.219(2) |
| 60. | N(1)-C(2) | 1.3344(15) |
| 61. | N(1)-C(6) | 1.3454(15) |
| 62. | C(2)-C(3) | 1.3817(17) |
| 63. | C(3)-C(4) | 1.3931(16) |
| 64. | C(4)-C(5) | 1.3950(16) |
| 65. | C(4)-C(7) | 1.5247(16) |
| 66. | C(5)-C(6) | 1.3800(17) |
| 67. | C(7)-C(8) | 1.514(2) |
| 68. | C(7)-C(10) | 1.529(2) |
| 69. | C(7)-C(9) | 1.5418(19) |
| 70. | | |
| 71. | O(1)-Cu(1)-O(1)#1 | 180.0 |
| 72. | O(1)-Cu(1)-N(1) | 90.22(4) |
| 73. | O(1)#1-Cu(1)-N(1) | 89.78(4) |
| 74. | O(1)-Cu(1)-N(1)#1 | 89.78(4) |
| 75. | O(1)#1-Cu(1)-N(1)#1 | 90.22(4) |
| 76. | N(1)-Cu(1)-N(1)#1 | 180.0 |
| 77. | C(1)-O(1)-Cu(1) | 107.91(8) |
| 78. | C(2)-N(1)-C(6) | 117.29(10) |
| 79. | C(2)-N(1)-Cu(1) | 121.40(8) |
| 80. | C(6)-N(1)-Cu(1) | 121.30(8) |
| 81. | O(2)-C(1)-O(1) | 125.61(13) |
| 82. | N(1)-C(2)-C(3) | 123.17(11) |
| 83. | C(2)-C(3)-C(4) | 120.12(11) |
| 84. | C(3)-C(4)-C(5) | 116.36(11) |
| 85. | C(3)-C(4)-C(7) | 122.95(11) |
| 86. | C(5)-C(4)-C(7) | 120.68(10) |
| 87. | C(6)-C(5)-C(4) | 120.17(11) |

| | | |
|---|---|---|
| 88. | N(1)-C(6)-C(5) | 122.87(11) |
| 89. | C(8)-C(7)-C(4) | 112.54(11) |
| 90. | C(8)-C(7)-C(10) | 110.86(16) |
| 91. | C(4)-C(7)-C(10) | 108.47(11) |
| 92. | C(8)-C(7)-C(9) | 107.96(14) |
| 93. | C(4)-C(7)-C(9) | 109.33(11) |
| 94. | C(10)-C(7)-C(9) | 107.55(13) |

95. _____

96. Symmetry transformations used to generate equivalent atoms:

97. #1 -x+2,-y+1,-z

98. Table 4. Anisotropic displacement parameters ($Å^2 x\ 10^3$) for tButPy. The anisotropic

99. displacement factor exponent takes the form: $-2\pi^2[\ h^2\ a^{*2}U^{11} + ...\ + 2\ h\ k\ a^*\ b^*\ U^{12}\ ]$

100.

| 101. | $U^{11}$ | $U^{22}$ | $U^{33}$ | $U^{23}$ | $U^{13}$ | $U^{12}$ |
|---|---|---|---|---|---|---|
| 102. | | | | | | |
| 103. Cu(1) | 29(1) | 19(1) | 37(1) | -3(1) | -16(1) | 1(1) |
| 104. O(1) | 37(1) | 28(1) | 44(1) | -3(1) | -21(1) | 0(1) |
| 105. O(2) | 46(1) | 49(1) | 63(1) | -18(1) | -14(1) | 4(1) |
| 106. N(1) | 30(1) | 22(1) | 35(1) | -5(1) | -14(1) | 1(1) |
| 107. C(1) | 36(1) | 36(1) | 43(1) | -2(1) | -18(1) | -8(1) |
| 108. C(2) | 32(1) | 23(1) | 34(1) | -6(1) | -16(1) | 4(1) |
| 109. C(3) | 28(1) | 28(1) | 33(1) | -7(1) | -14(1) | 3(1) |
| 110. C(4) | 30(1) | 24(1) | 27(1) | -7(1) | -12(1) | 0(1) |
| 111. C(5) | 33(1) | 21(1) | 44(1) | -6(1) | -17(1) | 3(1) |
| 112. C(6) | 28(1) | 24(1) | 48(1) | -6(1) | -16(1) | 3(1) |
| 113. C(7) | 34(1) | 27(1) | 37(1) | -6(1) | -13(1) | -4(1) |
| 114. C(8) | 36(1) | 42(1) | 120(2) | -10(1) | -26(1) | -4(1) |
| 115. C(9) | 58(1) | 39(1) | 50(1) | -19(1) | -22(1) | -6(1) |
| 116. C(10) | 78(1) | 43(1) | 33(1) | -2(1) | -14(1) | -22(1) |

117.

Table 5. Hydrogen coordinates ( x $10^4$) and isotropic displacement parameters ($Å^2$x $10^{-3}$) for tButPy.

| | x | y | z | U(eq) |
|---|---|---|---|---|
| H(1A) | 8823 | 5849 | -3406 | 47 |
| H(2A) | 5937 | 4157 | 825 | 35 |
| H(3A) | 3845 | 1795 | 1960 | 35 |
| H(5A) | 8235 | -1276 | 2360 | 39 |
| H(6A) | 10191 | 1178 | 1273 | 41 |
| H(8A) | 1934 | -391 | 3717 | 105 |
| H(8B) | 1670 | -2313 | 3671 | 105 |
| H(8C) | 2485 | -777 | 2070 | 105 |
| H(9A) | 5268 | -2504 | 1118 | 70 |
| H(9B) | 4434 | -4041 | 2715 | 70 |
| H(9C) | 6547 | -3275 | 2152 | 70 |
| H(10A) | 3993 | -1623 | 5362 | 81 |
| H(10B) | 5778 | -2749 | 4695 | 81 |
| H(10C) | 3660 | -3506 | 5267 | 81 |

Table 6. Torsion angles [°] for tButPy.

| | |
|---|---|
| Cu(1)-O(1)-C(1)-O(2) | 1.10(17) |
| C(6)-N(1)-C(2)-C(3) | 1.15(18) |
| Cu(1)-N(1)-C(2)-C(3) | -179.19(9) |
| N(1)-C(2)-C(3)-C(4) | -0.84(18) |
| C(2)-C(3)-C(4)-C(5) | -0.38(17) |
| C(2)-C(3)-C(4)-C(7) | 178.40(11) |
| C(3)-C(4)-C(5)-C(6) | 1.23(18) |
| C(7)-C(4)-C(5)-C(6) | -177.57(11) |
| C(2)-N(1)-C(6)-C(5) | -0.24(19) |
| Cu(1)-N(1)-C(6)-C(5) | -179.90(10) |
| C(4)-C(5)-C(6)-N(1) | -1.0(2) |
| C(3)-C(4)-C(7)-C(8) | 5.6(2) |
| C(5)-C(4)-C(7)-C(8) | -175.65(15) |
| C(3)-C(4)-C(7)-C(10) | -117.41(14) |
| C(5)-C(4)-C(7)-C(10) | 61.32(16) |
| C(3)-C(4)-C(7)-C(9) | 125.59(13) |
| C(5)-C(4)-C(7)-C(9) | -55.69(15) |

Symmetry transformations used to generate equivalent atoms:

#1 -x+2,-y+1,-z

Table 7. Hydrogen bonds for tButPy [Å and °].

| D-H...A | d(D-H) | d(H...A) | d(D...A) | <(DHA) |
|---|---|---|---|---|

## 8. Powder XRD of copper films of EtHex and 3ButPy-EtHex

Powder XRD was performed on selected copper films. As shown in Figure S1-11, the (111), (200) and (220) copper peaks are found at 43.6, 50.8 and 74.4° while the weak peak at 36° shows that the films have marginal levels of $Cu_2O$ present.

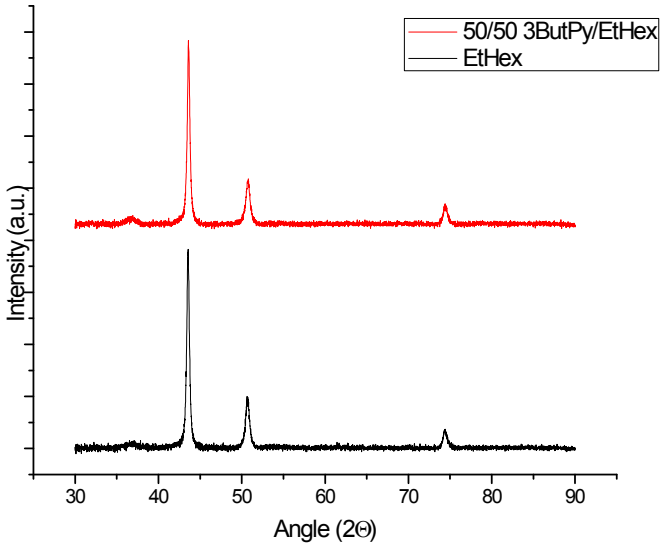


**Figure SI_11.** Powder XRD of films formed from *EtHex* and 50/50 *3ButPy* /*EtHex.*

(1) APEX Software Suite v.2012; Bruker AXS: Madison, WI, **2005**.

(2) R. Blessing, *Acta Cryst.* **1995**, *A51*, 33.

(3) G. M. Sheldrick, *Acta Cryst.* **2008**, *A64*, 112.

(4) D.F. Evans, *J. Chem. Soc.,* **1959**, 2003.

(5) R.L. Martin, H. Waterman J. Chem Soc. **1959**, 2960.